Proceedings of the 2010 IEEE
International Conference on Robotics and Biomimetics
December 14-18, 2010, Tianjin, China

Sensory Feedback Attitude Control for a Grasped Object by a Multi-Fingered Hand-Arm System

Akihiro Kawamura, Kenji Tahara, Ryo Kurazume and Tsutomu Hasegawa

***Abstract*— This paper proposes a novel method for stable grasping and attitude regulation of an object using a multi-fingered hand-arm system. The proposed method is based on a simple sensory-feedback control using the information of an object attitude, and any mathematically complicated computation, such as calculation of inverse dynamics and kinematics, are not required. In addition, the stability of the overall system applied this method is verified. Firstly, nonholonomic rolling constraints between a multi-fingered hand-arm system and an object are formulated. Then, a novel control method for stable grasping and attitude regulation of the grasped object is proposed. It is assumed that information of the attitude of the object is available in real time by external sensors, such as vision, force, tactile sensors, and so on. Next, the stability of the overall system is verified by analyzing the closed-loop dynamics. Finally, it is demonstrated through numerical simulations that our proposed method enables to grasp the object with arbitrary shape, and regulate the attitude of the object stably.**

I. Introduction

A multi-fingered hand-arm system has been expected to accomplish a dexterous grasping like a human hand. Robots with this system will be able to perform various manipulation tasks even in an unknown environment in stable. Aiming at this target, many robotic systems and control methods for grasping and manipulation of an object have been proposed [1–5]. Especially, several methods for grasping and manipulation using rolling constraints have been reported [6–9]. However, most of these methods are based on inverse kinematics and dynamics calculations, and require detailed object information such as a mass and a shape of an object in advance. In contrast, Arimoto *et al.* proposed a dynamic object grasping method [10–13] which requires neither any object information nor inverse dynamics and kinematics calculations. Furthermore, the stability of the overall system is verified theoretically. However, this method has just treated stable grasping, and the manipulation of the grasped object has not been considered.

In our previous work, we have proposed a dynamic stable grasping method for an arbitrary polyhedral shaped object [14]. In addition to this method, this paper proposes a novel object manipulation method to regulate the attitude of the grasped object using a multi-fingered hand-arm system with soft hemispherical fingertips. This method accomplishes a desired attitude control of the object using the object attitude information from some external sensors. No other information of the object grasped such as the mass and the shape of the object, and inverse kinematics and dynamics calculations are required in the proposed method. Firstly, we formulate a nonholonomic constraint between the multi-fingered hand-arm system and the object surface which is constrained by rolling and area contact with each fingertip. Arimoto *et al.* [10–13] has proposed a proper expression of the nonholonomic constraint for rolling contact which can take a dynamic equation of motion into account. However, this method is restricted for the case that an object has two flat and parallel surfaces. We expand the constraint for an arbitrary polyhedral shaped object and an arbitrary number of fingers. Secondly, we derive Lagrange's equation of motion for the overall system, and propose a new control signal. Finally, it is verified that the proposed method enables to regulate the attitude control of the object through numerical simulations.

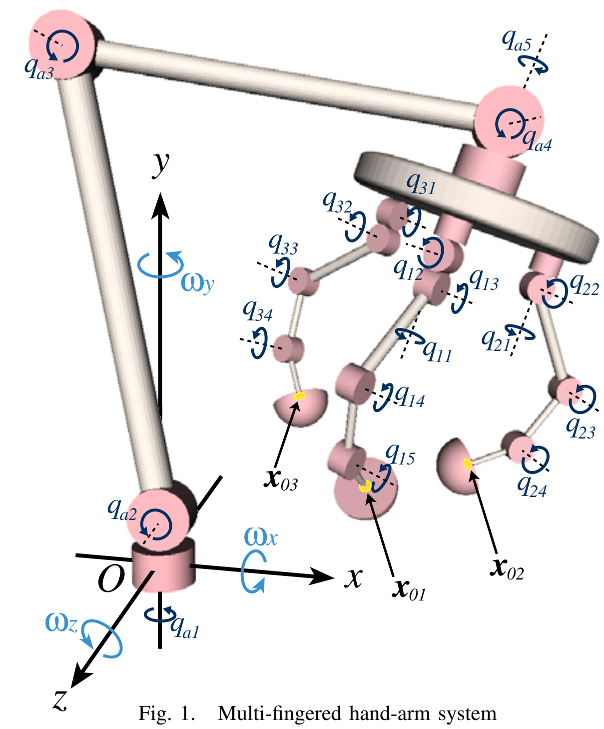

Fig. 1. Multi-fingered hand-arm system

This work was partially supported by "the Kyushu University Research Superstar Program (SSP)", based on the budget of Kyushu University allocated under President's initiative.

A. Kawamura is with the Graduate School of Information Science and Electrical Engineering, Kyushu University, Fukuoka, 819-0395, JAPAN kawamura@irvs.is.kyushu-u.ac.jp

K. Tahara is with the Institute for Advanced Study, Kyushu University, Fukuoka, 819-0395, JAPAN tahara@ieee.org

R. Kurazume and T. Hasegawa are with the Faculty of Information Science and Electrical Engineering, Kyushu University, Fukuoka, 819-0395, JAPAN {kurazume, hasegawa}@ait.kyushu-u.ac.jp

II. A Multi Fingered Hand Arm System

In this section, we define a model of a hand-arm system composed of an arm and a multi-fingered hand. An example of the multi-fingered hand-arm system treated here is illustrated in Fig. 1. This system has an arbitrary number of d.o.f.s which is enough to grasp and regulate the object attitude. Assume that all fingertips maintain rolling and area contact with the object surfaces, and do not slip and detach from the surfaces during manipulation. In addition, the fingertips roll within the ranges of hemisphere surfaces, and they do not deviate from each contact surface. Note that the gravity effect is ignored in this paper in order to have a physical insight into analyzing physical interaction and stability of the system. As shown in Fig. 1, the symbol O denotes the origin of Cartesian coordinates, and $\boldsymbol{x}_{0i} \in \mathbb{R}^3$ is the center of each contact area. Hereafter, the subscript of i refers to the ith finger in all equations. The number of d.o.f.s of the arm and the ith finger are N_a and N_i, respectively. The joint angle of the arm is expressed by $\boldsymbol{q}_a \in \mathbb{R}^{N_a}$. Similarly, each joint angle of the ith finger is expressed by $\boldsymbol{q}_{0i} \in \mathbb{R}^{\mathrm{N}_i}$. $\boldsymbol{q}$ denotes the joint angles of the arm and all the fingers $\left(= (\boldsymbol{q}_a, \boldsymbol{q}_{01}, \boldsymbol{q}_{02}, ..., \boldsymbol{q}_{0N})^{\mathrm{T}}\right)$. N is the number of the fingers. As shown in Fig. 2, $\boldsymbol{x}_i \in \mathbb{R}^3$ is the center of the contact area, and the symbol $O_{c.m.}$ denotes the center of the object mass and the origin of local coordinates. Its position in Cartesian coordinates is expressed as $\boldsymbol{x} = (x, y, z)^{\mathrm{T}} \in \mathbb{R}^3$. Instantaneous rotational axis of the object at $O_{c.m.}$ in Cartesian coordinates is expressed by $\boldsymbol{\omega} = (\omega_x, \omega_y, \omega_z)^{\mathrm{T}} \in \mathbb{R}^3$.

A. Rolling constraints

The attitude of the object in Cartesian coordinates can be expressed by the rotational matrix $\boldsymbol{R}$ such that

$$\boldsymbol{R} \;=\; (\boldsymbol{r}_X, \boldsymbol{r}_Y, \boldsymbol{r}_Z) \;\in SO(3), \tag{1}$$

where $\boldsymbol{r}_X, \boldsymbol{r}_Y, \boldsymbol{r}_Z \in \mathbb{R}^3$ are mutually orthonormal vectors on the object frame. It is known that this rotational matrix is one of the members of the group $SO(3)$. In addition to this, we define contact frames at the center of each contact area as follows:

$$\boldsymbol{R}{\cdot}\boldsymbol{R}_{Ci} \;=\; (\boldsymbol{C}_{iX}, \boldsymbol{C}_{iY}, \boldsymbol{C}_{iZ}), \tag{2}$$

where $\boldsymbol{R}_{Ci}$ is the rotational matrix between the object frame to the contact frames, and $\boldsymbol{C}_{iY}$ is a unit vector normal to the contact surface.

Now, the rolling constraints are expressed such that the velocity of the center of the contact area on the fingertip, should equal to the velocity of the center of the contact area on the object surface. They are given as follows:

$$\begin{bmatrix} \boldsymbol{C}_{iX}^{\mathrm{T}} \\ \boldsymbol{C}_{iZ}^{\mathrm{T}} \end{bmatrix} \boldsymbol{v}_i = \begin{bmatrix} \dot{X}_i \\ \dot{Z}_i \end{bmatrix}, \tag{3}$$

where

$$\boldsymbol{v}_i \;=\; \Delta r_i \left(\dot{\boldsymbol{C}}_{iY} - \boldsymbol{\omega}_i \times \boldsymbol{C}_{iY}\right) \tag{4}$$

$$X_i \;=\; -\boldsymbol{C}_{iX}^{\top}(\boldsymbol{x} - \boldsymbol{x}_{0i}) \tag{5}$$

$$Z_i \;=\; -\boldsymbol{C}_{iZ}^{\top}(\boldsymbol{x} - \boldsymbol{x}_{0i}). \tag{6}$$

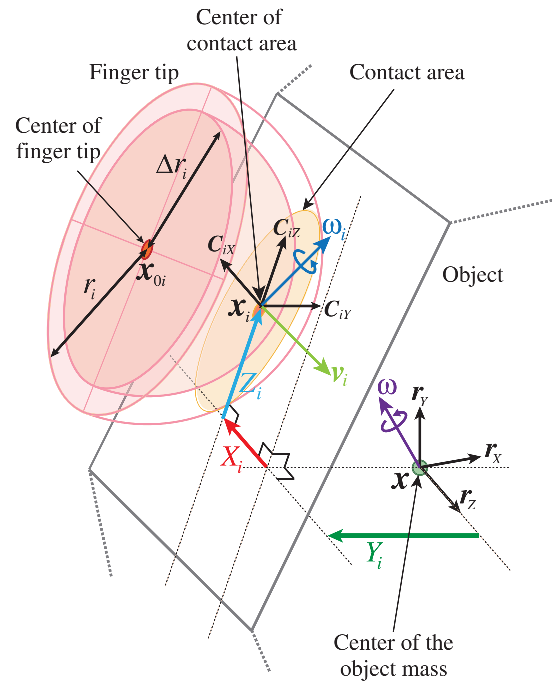

Fig. 2. Contact model between a fingertip and an object surface at the center of a contact area

$\boldsymbol{v}_i$ is on the tangential plane at the center of the contact area (now, they are surfaces of the object). $\boldsymbol{\omega}_i \in \mathbb{R}^3$ is the attitude angular velocity vector for each robotic finger on the contact frames, r_i is the radius of each fingertip, and Δr_i is the perpendicular distance between the center of the fingertips and the contact surfaces (see Fig. 2). Equation (3) denotes nonholonomic rolling constraints on the object surfaces. This constraint is linear with respect to each velocity vector, and thereby it can be expressed as Pfaffian constraints in the following form:

$$\begin{bmatrix} \boldsymbol{X}_{iq} \\ \boldsymbol{Z}_{iq} \end{bmatrix} \dot{\boldsymbol{q}} + \begin{bmatrix} \boldsymbol{X}_{ix} \\ \boldsymbol{Z}_{ix} \end{bmatrix} \dot{\boldsymbol{x}} + \begin{bmatrix} \boldsymbol{X}_{i\omega} \\ \boldsymbol{Z}_{i\omega} \end{bmatrix} \boldsymbol{\omega} = \boldsymbol{0}, \tag{7}$$

where

$$\left[\begin{array}{l} \boldsymbol{X}_{iq} = \Delta r_i \boldsymbol{C}_{iZ}^{\mathrm{T}} \boldsymbol{J}_{\Omega i} - \boldsymbol{C}_{iX}^{\mathrm{T}} \boldsymbol{J}_{0i} \\ \boldsymbol{X}_{ix} = \boldsymbol{C}_{iX}^{\mathrm{T}} \\ \boldsymbol{X}_{i\omega} = \{\boldsymbol{C}_{iX} \times (\boldsymbol{x} - \boldsymbol{x}_{0i})\}^{\mathrm{T}} - \Delta r_i \boldsymbol{C}_{iZ}^{\mathrm{T}} \\ \boldsymbol{Z}_{iq} = -\Delta r_i \boldsymbol{C}_{iX}^{\mathrm{T}} \boldsymbol{J}_{\Omega i} - \boldsymbol{C}_{iZ}^{\mathrm{T}} \boldsymbol{J}_{0i} \\ \boldsymbol{Z}_{ix} = \boldsymbol{C}_{iZ}^{\mathrm{T}} \\ \boldsymbol{Z}_{i\omega} = \{\boldsymbol{C}_{iZ} \times (\boldsymbol{x} - \boldsymbol{x}_{0i})\}^{\mathrm{T}} + \Delta r_i \boldsymbol{C}_{iX}^{\mathrm{T}}, \end{array}\right. \tag{8}$$

and $\boldsymbol{J}_{\Omega_i} \in \mathbb{R}^{3\times\left(N_a + \sum_{i=1}^{N} N_i\right)}$ is the Jacobian matrix for the attitude angular velocities of the fingertips with respect to the joint angular velocity $\dot{\boldsymbol{q}} \in \mathbb{R}^{N_a + \sum_{i=1}^{N} N_i}$. $\boldsymbol{J}_{0i} \in \mathbb{R}^{3\times\left(N_a + \sum_{i=1}^{N} N_i\right)}$ is the Jacobian matrix for the center of the fingertip $\boldsymbol{x}_{0i}$ with respect to the joint angle, respectively.

B. Contact Model of Soft Finger-Tip

In this paper, the physical relationship between the deformation of the fingertip at the center of the contact area and its reproducing force is given on the basis of lumped-parameterized model proposed by Arimoto *et al* [10]. The reproducing force $f(\Delta r)$ in the normal direction to the object surface at the center of the contact area is given as follows:

$$\left[\begin{array}{l} f_i = \bar{f}_i + \xi_i \frac{d}{dt}(r_i - \Delta r_i) \\ \bar{f}_i = k(r_i - \Delta r_i)^2, \end{array}\right. \tag{9}$$

where k is a positive stiffness constant of the material of the fingertip. In the second term of the right-hand side of the upper equation of (9), $\xi_i(\Delta r_i)$ is a positive scalar function with respect to Δr_i. It indicates that the viscous force increases according to the expansion of the contact area.

Additionally, there are viscosities between fingertips and object surfaces in twist direction [15]. The energy dissipation function derived from the viscosities is expressed as follows:

$$T_{\omega i} = \frac{b_i}{2} ||\boldsymbol{C}_{iY}^{\mathrm{T}}(\boldsymbol{\omega} - \boldsymbol{\omega}_i)||^2, \tag{10}$$

where b_i is the coefficient of viscosity which depends on property of fingertips and the expansion of the contact area.

C. Overall Dynamics

The total kinetic energy for the overall system can be described as follows:

$$K = \frac{1}{2}\dot{\boldsymbol{q}}^{\mathrm{T}}\boldsymbol{H}\dot{\boldsymbol{q}} + \frac{1}{2}\dot{\boldsymbol{x}}^{\mathrm{T}}\boldsymbol{M}\dot{\boldsymbol{x}} + \frac{1}{2}\boldsymbol{\omega}^{\mathrm{T}}\boldsymbol{I}\boldsymbol{\omega}, \tag{11}$$

where $\boldsymbol{H} \in \mathbb{R}^{\left(N_a + \sum_{i=1}^N N_i\right)\times\left(N_a + \sum_{i=1}^N N_i\right)}$ is the inertia matrix for the arm and the fingers, $\boldsymbol{M} = \mathrm{diag}(m, m, m)$ is the mass of the object, $\boldsymbol{I} = \boldsymbol{R}\bar{\boldsymbol{I}}\boldsymbol{R}^{\mathrm{T}}$, and $\bar{\boldsymbol{I}} \in \mathbb{R}^{3\times3}$ is the inertia tensor for the object represented by the principal axes of inertia.

On the other hand, the total potential energy for the overall system is given as follows:

$$P = \sum_{i=1}^{N} P(\Delta r_i) = \sum_{i=1}^{N} \int_0^{r_i - \Delta r_i} \bar{f}_i(\Delta r_i)\, d\zeta, \tag{12}$$

where $P(\Delta r_i)$ is the elastic potential energy for each finger generated by the deformation of the fingertip. Lagrange's equation of motion is expressed by applying the variational principle as follows:

For the multi-fingered hand-arm system:

$$\boldsymbol{H}(\boldsymbol{q})\ddot{\boldsymbol{q}} + \left\{\frac{1}{2}\dot{\boldsymbol{H}}(\boldsymbol{q}) + \boldsymbol{S}(\boldsymbol{q}, \dot{\boldsymbol{q}})\right\}\dot{\boldsymbol{q}} + \sum_{i=1}^{N} \frac{\partial T_i}{\partial \dot{\boldsymbol{q}}}^{\mathrm{T}} + \sum_{i=1}^{N}\left(\boldsymbol{J}_{0i}^{\mathrm{T}}\boldsymbol{C}_{iY} f_i + \boldsymbol{X}_{iq}^{\mathrm{T}}\lambda_{iX} + \boldsymbol{Z}_{iq}^{\mathrm{T}}\lambda_{iZ}\right) = \boldsymbol{u}, \tag{13}$$

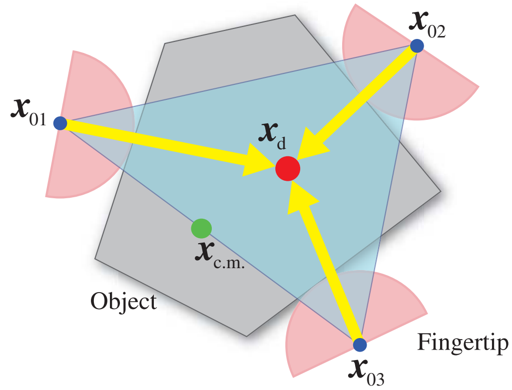

Fig. 3. Each center of fingertip approaches a centroid of a polyhedron made of them

For the object:

$$\boldsymbol{M}\ddot{\boldsymbol{x}} + \sum_{i=1}^{N}\left(-f_i\boldsymbol{C}_{iY} + \boldsymbol{X}_{ix}^{\mathrm{T}}\lambda_{iX} + \boldsymbol{Z}_{ix}^{\mathrm{T}}\lambda_{iZ}\right) = \boldsymbol{0} \tag{14}$$

$$\boldsymbol{I}\dot{\boldsymbol{\omega}} + \boldsymbol{\omega}\times\boldsymbol{I}\boldsymbol{\omega} + \sum_{i=1}^{N}\frac{\partial T_i}{\partial \boldsymbol{\omega}}^{\mathrm{T}} - \sum_{i=1}^{N}\{\boldsymbol{C}_{iY}\times(\boldsymbol{x} - \boldsymbol{x}_{0i})\}f_i + \sum_{i=1}^{N}\left(\boldsymbol{X}_{i\omega}^{\mathrm{T}}\lambda_{iX} + \boldsymbol{Z}_{i\omega}^{\mathrm{T}}\lambda_{iZ}\right) = \boldsymbol{0}, \tag{15}$$

where $\boldsymbol{S}(\boldsymbol{q}, \dot{\boldsymbol{q}})$ is skew-symmetric matrix, $\boldsymbol{u}$ is a vector of the input torque. In addition, λ_{iX} and λ_{iZ} denote Lagrange's multipliers.

III. Control Input

We propose a new attitude control method of an object for a multi fingered hand-arm system. This control signal is composed of two independent parts. One part performs stable grasping and the other part controls the attitude of the object. The control signal for stable grasping $\boldsymbol{u}_s$ is designed so that the center of each fingertip approaches a centroid of a polyhedron made of them [14] (see Fig. 3), and given as follows:

$$\boldsymbol{u}_s = \frac{f_d}{\sum_{i=1}^{N} r_i}\sum_{j=1}^{N}\boldsymbol{J}_{0j}^{\mathrm{T}}(\boldsymbol{x}_d - \boldsymbol{x}_{0j}) - \boldsymbol{C}\dot{\boldsymbol{q}} \tag{16}$$

$$\boldsymbol{x}_d = \frac{1}{N}\sum_{i=1}^{N}\boldsymbol{x}_{0i}, \tag{17}$$

where $\boldsymbol{C} \in \mathbb{R}^{\left(N_a + \sum_{i=1}^N N_i\right)\times\left(N_a + \sum_{i=1}^N N_i\right)} > 0$ is a positive definite diagonal matrix that expresses the damping gain for each finger, and f_d is the nominal desired grasping force.

Secondly, we show the simple and novel control signal for the attitude control of the object $\boldsymbol{u}_o$. The desired attitude of the object is expressed by the rotational matrix $\boldsymbol{R}_d =$

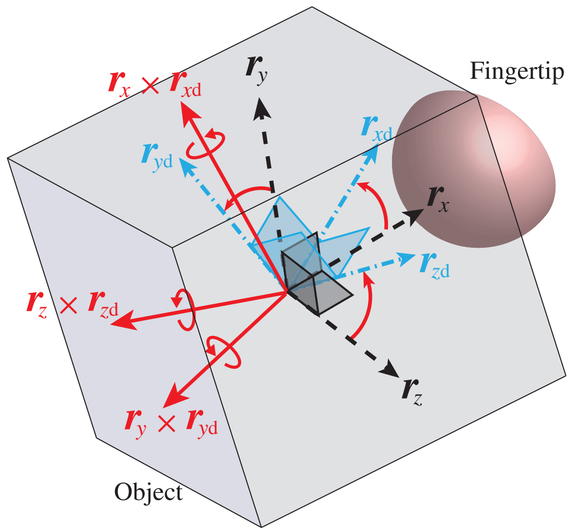

Fig. 4. $\boldsymbol{r}_x \times \boldsymbol{r}_{xd}$ is an error vector between a desired state and a present state with respect to the object attitude and those about y and z axes can be generated in the similar way

$(\boldsymbol{r}_{xd}, \boldsymbol{r}_{yd}, \boldsymbol{r}_{zd})$. The control signal for regulating the attitude of the object $\boldsymbol{u}_o$ is given as follows:

$$\begin{aligned}\boldsymbol{u}_o \;=\; & K_o \sum_{j=1}^{N} \boldsymbol{J}_{\Omega j}^{\mathrm{T}} \left\{(\boldsymbol{r}_x \times \boldsymbol{r}_{xd})\right. \\ & \left. + (\boldsymbol{r}_y \times \boldsymbol{r}_{yd}) + (\boldsymbol{r}_z \times \boldsymbol{r}_{zd})\right\}, \qquad (18)\end{aligned}$$

where $K_o > 0$ is a positive scalar constant. $\boldsymbol{r}_x \times \boldsymbol{r}_{xd}$ is an error vector between a desired state and a present state with respect to the object attitude. Namely, this error vector is zero if the object attitude coincides with the desired attitude. Eventually, the total control signal $\boldsymbol{u}$ is given as follows:

$$\boldsymbol{u} = \boldsymbol{u}_s + \boldsymbol{u}_o \qquad (19)$$

IV. Closed-Loop Dynamics

In this section, we show the closed-loop dynamics of the overall system. It is given from the Lagrange's equation of motion and the control signal as follows:
For the multi-fingered hand-arm system:

$$\begin{aligned}\boldsymbol{H}\ddot{\boldsymbol{q}} \;+\; & \left\{\frac{1}{2}\dot{\boldsymbol{H}} + \boldsymbol{S} + \boldsymbol{C}\right\}\dot{\boldsymbol{q}} + \sum_{i=1}^{N} \boldsymbol{J}_{0i}^{\mathrm{T}} \boldsymbol{C}_{iY} \Delta f_i \\ & + \sum_{i=1}^{N} \boldsymbol{X}_{iq}^{\mathrm{T}} \Delta\lambda_{iX} + \sum_{i=1}^{N} \boldsymbol{Z}_{iq}^{\mathrm{T}} \Delta\lambda_{iZ} + \sum_{i=1}^{N} \frac{\partial T}{\partial \dot{\boldsymbol{q}}}^{\mathrm{T}} \\ & + \sum_{i=1}^{N} A \boldsymbol{J}_{\Omega i}^{\mathrm{T}} (\boldsymbol{x}_i - \boldsymbol{x}_{0i}) \times (\boldsymbol{x}_d - \boldsymbol{x}_{0i}) \\ & + \sum_{i=1}^{N} K_o \boldsymbol{C}_{iY}^{\mathrm{T}} \boldsymbol{B} \boldsymbol{J}_{\Omega i}^{\mathrm{T}} \boldsymbol{C}_{iY} \\ & + \sum_{i=1}^{N} \left\{-\frac{K_o}{\Delta r_i} \boldsymbol{J}_{0i}^{\mathrm{T}} (\boldsymbol{B} \times \boldsymbol{C}_{iY})\right\} = \boldsymbol{0}, \qquad (20)\end{aligned}$$

For the object:

$$\begin{aligned}\boldsymbol{M}\ddot{\boldsymbol{x}} + & \sum_{i=1}^{N} \left(-\Delta f_i \boldsymbol{C}_{iY} + \boldsymbol{X}_{ix}^{\mathrm{T}} \Delta\lambda_{iX} + \boldsymbol{Z}_{ix}^{\mathrm{T}} \Delta\lambda_{iZ}\right) \\ & - \sum_{i=1}^{N} \left\{A(\boldsymbol{x}_d - \boldsymbol{x}_{0i}) - \frac{K_o}{\Delta r_i}(\boldsymbol{B} \times \boldsymbol{C}_{iY})\right\} = \boldsymbol{0} \quad (21)\end{aligned}$$

$$\begin{aligned}& \boldsymbol{I}\dot{\boldsymbol{\omega}} + \boldsymbol{\omega} \times \boldsymbol{I}\boldsymbol{\omega} - \sum_{i=1}^{N} \{\boldsymbol{C}_{iY} \times (\boldsymbol{x} - \boldsymbol{x}_{0i})\}\Delta f_i \\ & + \sum_{i=1}^{N} \left(\boldsymbol{X}_{i\omega}^{\mathrm{T}} \Delta\lambda_{iX} + \boldsymbol{Z}_{i\omega}^{\mathrm{T}} \Delta\lambda_{iZ}\right) + \sum_{i=1}^{N} \frac{\partial T}{\partial \boldsymbol{\omega}}^{\mathrm{T}} \\ & + \sum_{i=1}^{N} (\boldsymbol{x} - \boldsymbol{x}_i) \times \left\{A(\boldsymbol{x}_d - \boldsymbol{x}_{0i}) - \frac{K_o}{\Delta r_i}(\boldsymbol{B} \times \boldsymbol{C}_{iY})\right\} \\ & = \boldsymbol{0}, \qquad (22)\end{aligned}$$

where

$$\left[\begin{array}{l} A = \frac{f_d}{\sum_{j=1}^{N} \Delta r_j} \\ \boldsymbol{B} = (\boldsymbol{r}_{xd} \times \boldsymbol{r}_x) + (\boldsymbol{r}_{yd} \times \boldsymbol{r}_y) + (\boldsymbol{r}_{zd} \times \boldsymbol{r}_z) \\ \Delta f_i = f_i - A\boldsymbol{C}_{iY}^{\mathrm{T}}(\boldsymbol{x}_d - \boldsymbol{x}_{0i}) \\ \Delta\lambda_{iX} = \lambda_{iX} + A\boldsymbol{C}_{iX}^{\mathrm{T}}(\boldsymbol{x}_d - \boldsymbol{x}_{0i}) + \frac{K_o}{\Delta r_i}\boldsymbol{C}_{iZ}^{\mathrm{T}}\boldsymbol{B} \\ \Delta\lambda_{iX} = \lambda_{iZ} + A\boldsymbol{C}_{iZ}^{\mathrm{T}}(\boldsymbol{x}_d - \boldsymbol{x}_{0i}) - \frac{K_o}{\Delta r_i}\boldsymbol{C}_{iX}^{\mathrm{T}}\boldsymbol{B} \end{array}\right. \qquad (23)$$

Now, an output vector of the overall system is given as follows:

$$\dot{\boldsymbol{\Lambda}} = \left(\dot{\boldsymbol{q}}^{\mathrm{T}}, \dot{\boldsymbol{x}}^{\mathrm{T}}, \boldsymbol{\omega}^{\mathrm{T}}\right)^{\mathrm{T}}. \qquad (24)$$

By taking a sum of the inner product of (24) and the closed loop dynamics expressed by (20), (21) and (22), we obtain

$$\frac{d}{dt}E = -\dot{\boldsymbol{q}}^{\mathrm{T}}\boldsymbol{C}\dot{\boldsymbol{q}} - \sum_{i=1}^{N}\left(T_i + \xi\Delta\dot{r}_i^2\right) - D \le 0 \qquad (25)$$

$$E = K + V + \Delta P \ge 0 \qquad (26)$$

$$K = \frac{1}{2}\dot{\boldsymbol{q}}^{\mathrm{T}}\boldsymbol{H}\dot{\boldsymbol{q}} + \frac{1}{2}\dot{\boldsymbol{x}}^{\mathrm{T}}\boldsymbol{M}\dot{\boldsymbol{x}} + \frac{1}{2}\boldsymbol{\omega}^{\mathrm{T}}\boldsymbol{I}\boldsymbol{\omega} \qquad (27)$$

$$V = V_s + V_o \qquad (28)$$

$$\begin{aligned}V_s = \frac{A}{2}\Big\{&(\boldsymbol{x}_{01} - \boldsymbol{x}_{02})^2 + (\boldsymbol{x}_{02} - \boldsymbol{x}_{03})^2 \\ & + \dots + (\boldsymbol{x}_{0N} - \boldsymbol{x}_{01})^2\Big\} \qquad (29)\end{aligned}$$

$$\begin{aligned}V_o = \frac{NK_o}{2}\Big\{&(\boldsymbol{r}_x - \boldsymbol{r}_{xd})^2 + (\boldsymbol{r}_y - \boldsymbol{r}_{yd})^2 \\ & + (\boldsymbol{r}_z - \boldsymbol{r}_{zd})^2\Big\} \qquad (30)\end{aligned}$$

$$\Delta P = \sum_{i=1}^{N} \int_0^{\delta r_i} \left\{\bar{f}_i(\Delta r_{di} + \phi) - \bar{f}_i(\Delta r_{di})\right\} d\phi, \qquad (31)$$

where

$$\delta r_i \;=\; \Delta r_{di} - \Delta r_i \qquad (32)$$

$$\begin{aligned}D \;=\; & \sum_{i=1}^{N} \frac{K_o}{\Delta r_i}\Big\{(\boldsymbol{x} - \boldsymbol{x}_{0i})^{\mathrm{T}}\left(\boldsymbol{R}\boldsymbol{R}_d^{\mathrm{T}} - \boldsymbol{R}_d\boldsymbol{R}^{\mathrm{T}}\right)\dot{\boldsymbol{C}}_{iY} \\ + \; & (\dot{\boldsymbol{x}} - \dot{\boldsymbol{x}}_{0i})^{\mathrm{T}}\left(\boldsymbol{R}\boldsymbol{R}_d^{\mathrm{T}} - \boldsymbol{R}_d\boldsymbol{R}^{\mathrm{T}}\right)\boldsymbol{C}_{iY}\Big\}. \qquad (33)\end{aligned}$$

In (32), Δr_{di} is Δr_i when f_i equals to f_d. V plays a role of an artificial potential energy arisen from the control input. In (25), all the terms except D are semi-negative. The term of D can be ensured the boundedness by considering $||\boldsymbol{R}|| = ||\boldsymbol{R}_d|| = 1$ and the boundedness of $\frac{d}{dt}\left\{(\boldsymbol{x}-\boldsymbol{x}_{0i})^{\mathrm{T}}\boldsymbol{C}_{iY}\right\}$. Therefore, the damping gain $\boldsymbol{C}$ is configured to make $\dot{E} \leq 0$. In addition, (26) can be satisfied because K, V and ΔP are positive as far as $0 \leq \Delta r_{di} - \delta r_i < r_i$. Eventually, (25) and (26) yield

$$\int_0^{\infty}\left(\dot{\boldsymbol{q}}^{\mathrm{T}}\boldsymbol{C}\dot{\boldsymbol{q}} + \sum_{i=1}^{N}\xi\Delta\dot{r}_i^2\right)dt \leq E(0) - E(t) \leq E(0), \tag{34}$$

Equation (34) shows that the joint angular velocity $\dot{\boldsymbol{q}}(t)$ is squared integrable over time $t \in [0,\infty)$. It shows that $\dot{\boldsymbol{q}}(t) \in L^2(0,\infty)$. Considering the constraints shown by (4) and (5), it is clear that $\dot{\boldsymbol{x}} \in L^2(0,\infty)$ and $\boldsymbol{\omega} \in L^2(0,\infty)$. Thereby, the output of the overall system $\dot{\boldsymbol{\Lambda}}(t)$ is uniformly continuous and it is shown that $\dot{\boldsymbol{\Lambda}} \to \boldsymbol{0}$ and $\ddot{\boldsymbol{\Lambda}} \to \boldsymbol{0}$ when $t \to \infty$ [11]. Therefore, it is obvious that the sum of the nominal external forces applied to the hand-arm system and the object $\boldsymbol{\Delta}\lambda_{\infty}$ is converged to zero. Namely,

$$\boldsymbol{\Delta}\lambda_{\infty} = (\boldsymbol{\Delta}\lambda_{\boldsymbol{q}}, \boldsymbol{\Delta}\lambda_{\boldsymbol{x}}, \boldsymbol{\Delta}\lambda_{\boldsymbol{\omega}}) \to \boldsymbol{0}, \tag{35}$$

where

$$\begin{aligned}\boldsymbol{\Delta}\lambda_{\boldsymbol{q}} =& \sum_{i=1}^{N}\left(\boldsymbol{J}_{0i}^{\mathrm{T}}\boldsymbol{C}_{iY}\Delta f_i + \boldsymbol{X}_{iq}^{\mathrm{T}}\Delta\lambda_{iX} + \boldsymbol{Z}_{iq}^{\mathrm{T}}\Delta\lambda_{iZ}\right)\\ &+ \sum_{i=1}^{N} A\boldsymbol{J}_{\Omega i}^{\mathrm{T}}(\boldsymbol{x}_i - \boldsymbol{x}_{0i}) \times (\boldsymbol{x}_d - \boldsymbol{x}_{0i})\\ &+ \sum_{i=1}^{N}\left\{K_o\boldsymbol{C}_{iY}^{\mathrm{T}}\boldsymbol{B}\boldsymbol{J}_{\Omega i}^{\mathrm{T}}\boldsymbol{C}_{iY} - \frac{K_o}{\Delta r_i}\boldsymbol{J}_{0i}^{\mathrm{T}}(\boldsymbol{B}\times\boldsymbol{C}_{iY})\right\}\end{aligned} \tag{36}$$

$$\begin{aligned}\boldsymbol{\Delta}\lambda_{\boldsymbol{x}} =& \sum_{i=1}^{N}\left(-\Delta f_i\boldsymbol{C}_{iY} + \boldsymbol{X}_{ix}^{\mathrm{T}}\Delta\lambda_{iX} + \boldsymbol{Z}_{ix}^{\mathrm{T}}\Delta\lambda_{iZ}\right)\\ &- \sum_{i=1}^{N}\left\{A(\boldsymbol{x}_d - \boldsymbol{x}_{0i}) - \frac{K_o}{\Delta r_i}(\boldsymbol{B}\times\boldsymbol{C}_{iY})\right\}\end{aligned} \tag{37}$$

$$\begin{aligned}\boldsymbol{\Delta}\lambda_{\boldsymbol{\omega}} =& -\sum_{i=1}^{N}\{\boldsymbol{C}_{iY}\times(\boldsymbol{x}-\boldsymbol{x}_{0i})\}\Delta f_i\\ &+ \sum_{i=1}^{N}\left(\boldsymbol{X}_{i\omega}^{\mathrm{T}}\Delta\lambda_{iX} + \boldsymbol{Z}_{i\omega}^{\mathrm{T}}\Delta\lambda_{iZ}\right)\\ &+ \sum_{i=1}^{N}(\boldsymbol{x}-\boldsymbol{x}_i)\times\left\{A(\boldsymbol{x}_d - \boldsymbol{x}_{0i}) - \frac{K_o}{\Delta r_i}(\boldsymbol{B}\times\boldsymbol{C}_{iY})\right\},\end{aligned} \tag{38}$$

and $\boldsymbol{\Delta}\lambda_{\boldsymbol{q}}$ denotes an external force applied to each joint of the hand-arm system, and $\boldsymbol{\Delta}\lambda_{\boldsymbol{x}}$ and $\boldsymbol{\Delta}\lambda_{\boldsymbol{\omega}}$ are also external forces applied to the object.

As a consequence, it is shown the desired attitude of the object is realized stably, because each nominal external force and velocity becomes zero.

TABLE I

PHYSICAL PARAMETERS

Triple-fingered hand-arm system

1st link length l_{a1}	1.300[m]
2nd link length l_{a2}	1.000[m]
3rd link length l_{a3}	0.175[m]
1st link length l_{i1}	0.300[m]
2nd link length l_{i2}	0.200[m]
3rd link length l_{i3}	0.140[m]
1st mass center l_{ga1}	0.650[m]
2nd mass center l_{ga2}	0.500[m]
3rd mass center l_{ga3}	0.0875[m]
1st mass center l_{gi1}	0.150[m]
2nd mass center l_{gi2}	0.100[m]
3rd mass center l_{gi3}	0.070[m]
1st mass m_{a1}	1.300[kg]
2nd mass m_{a2}	1.000[kg]
3rd mass m_{a3}	0.400[kg]
1st mass m_{i1}	0.250[m]
2nd mass m_{i2}	0.150[m]
3rd mass m_{i3}	0.100[m]
1st Inertia $\boldsymbol{I}_{a1}$	$\mathrm{diag}(7.453, 7.453, 0.260)\times10^{-1}$[kg·m^2]
2nd Inertia $\boldsymbol{I}_{a2}$	$\mathrm{diag}(3.397, 3.397, 0.128)\times10^{-1}$[kg·m^2]
3rd Inertia $\boldsymbol{I}_{a3}$	$\mathrm{diag}(0.291, 0.291, 0.500)\times10^{-1}$[kg·m^2]
1st Inertia $\boldsymbol{I}_{i1}$	$\mathrm{diag}(7.725, 7.725, 0.450)\times10^{-3}$[kg·m^2]
2nd Inertia $\boldsymbol{I}_{i2}$	$\mathrm{diag}(2.060, 2.060, 0.120)\times10^{-3}$[kg·m^2]
3rd Inertia $\boldsymbol{I}_{i3}$	$\mathrm{diag}(0.538, 0.538, 0.031)\times10^{-3}$[kg·m^2]
Radius of fingertip r_i	0.070[m]
Stiffness coefficient k_i	1.000×10^5[N/m^2]
Damping function ξ_i	$1.000\times\left(r_i^2 - \Delta r_i^2\right)\pi$[Ns/m^2]

Object

Mass m	0.037[kg]
Y_1	0.092[m]
Y_2	0.048[m]
Y_3	0.048[m]
θ_{t1}	1.833[rad]
θ_{t2}	1.833[rad]
θ_{t3}	2.618[rad]
Inertia $\boldsymbol{I}$	$\mathrm{diag}(1.273, 0.193, 1.148)\times10^{-3}$[kg·m^2]

TABLE II

DESIRED GRASPING FORCE AND GAINS

f_d	10.0[N]
$\boldsymbol{C}_a$	$\mathrm{diag}(1.673, 1.085, 1.225, 0.463, 0.295)\times10^{-1}$[Ns·m/rad]
$\boldsymbol{C}_1$	$\mathrm{diag}(1.010, 1.095, 1.310, 0.535, 0.165)\times10^{-2}$[Ns·m/rad]
$\boldsymbol{C}_2$	$\mathrm{diag}(0.780, 1.300, 0.530, 0.165)\times10^{-2}$[Ns·m/rad]
$\boldsymbol{C}_3$	$\mathrm{diag}(1.065, 1.300, 0.530, 0.165)\times10^{-2}$[Ns·m/rad]
K_o	0.24

V. NUMERICAL SIMULATION

In this section, we report an example of these simulations. The robot used in this simulation is a triple-fingered hand-arm system. It consists of an arm part which has 5 d.o.f.s and a triple-fingered part which has one 5 d.o.f.s finger and two 4 d.o.f.s fingers. The grasped object is triangular prism, and the cross-section view of the object is shown in Fig. 5. Y_i is the distance from the center of the object mass $O_{c.m.}$ to the surface, and θ_{ti} is the external angle of the polygon parallel to the bottom of the object. The parameters of the triple-fingered hand-arm system and the object are shown

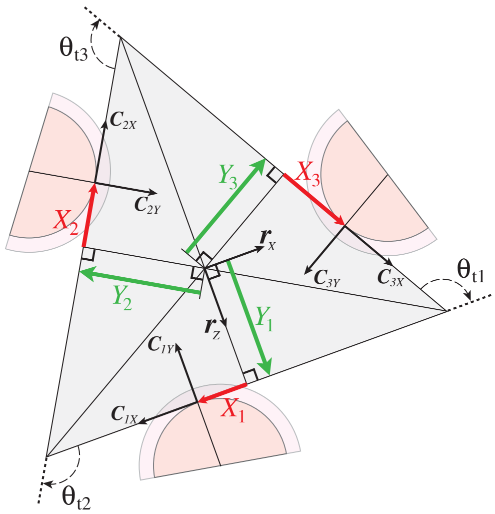

Fig. 5. Cross-section view of polygonal column

in Table I. Table II shows the desired nominal grasping force and gains. Figure 6 shows the transient responses of object frame and its desired frame, and we can see that the object frame $\boldsymbol{R} = (\boldsymbol{r}_x, \boldsymbol{r}_y, \boldsymbol{r}_z)$ converges to the desired frame $\boldsymbol{R}_d = (\boldsymbol{r}_{xd}, \boldsymbol{r}_{yd}, \boldsymbol{r}_{zd})$. Figures 7 and 8 show the elements of $\boldsymbol{\Delta}\lambda_\infty$ converges to zero. It is shown that the sum of the nominal external forces applied to the system and the object converges to zero. Figures 9 and 10 show the transient responses of $\dot{\boldsymbol{q}}$, $\dot{\boldsymbol{x}}$ and $\boldsymbol{\omega}$. We can confirm that the velocities of the overall system converge to zero. The results illustrate that the dynamic force/torque equibilium condition for immobilization of the object is realized with satisfying the desired attitude.

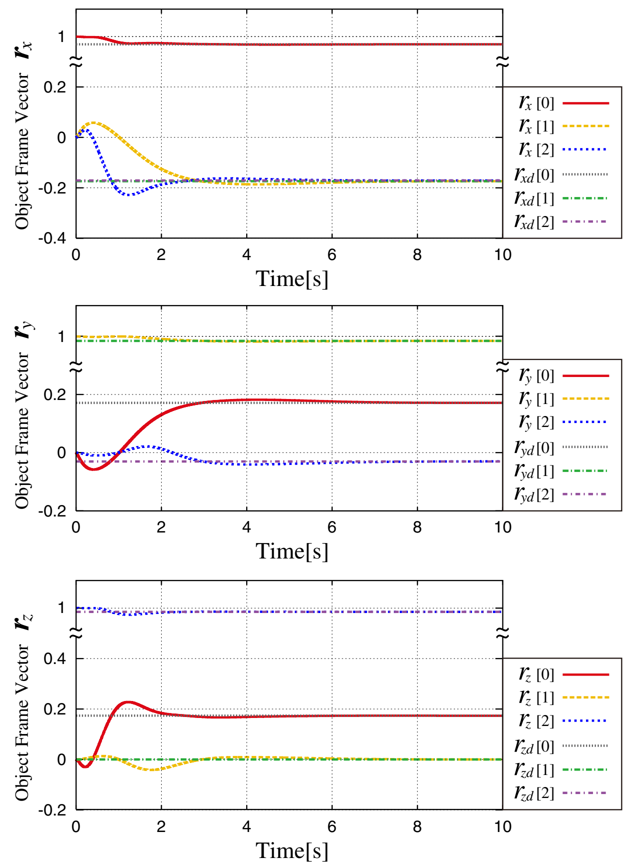

Fig. 6. Transient responses of the object frame $\boldsymbol{R} = (\boldsymbol{r}_x, \boldsymbol{r}_y, \boldsymbol{r}_z)$

VI. Conclusion

This paper presented the novel object attitude control method for an arbitrary polyhedral object by a multi-fingered hand-arm system. Firstly, the nonholonomic constraints of rolling and area contact were formulated, and proposed two control signals for stable grasping and attitude control. Next, the stability of the overall system with proposed method was verified by analyzing the closed-loop dynamics. Finally, it is verified that the proposed method realizes object attitude control stably through the numerical simulation result.

In the future works, we will conduct mechanical experiments to verify the usefulness of our proposed method. Furthermore, we will expand the proposed control scheme for an object with arbitrary smooth curved surfaces.

Acknowledgment

This work was partially supported by ”the Kyushu University Research Superstar Program (SSP)”, based on the budget of Kyushu University allocated under President’s initiative and Grant-in-Aid for JSPS Fellows.

References

[1] M. R. Cutkosky, *Grasping and Fine Manipulation*, Kluwer Academic, Dordrecht, Netherlands; 1985.

[2] R. M. Murray, Z. Li and S. S. Sastry, *Mathematical Introduction to Robotic Manipulation*, CRC Press, Boca Raton; 1994.

[3] K. B. Shimoga, “Robot grasp synthesis algorithms: A survey,” *Int. J. Robotics Research*, vol. 15, no. 3, pp. 230–266, 1996.

[4] A. M. Okamura, N. Smaby and M. R. Cutkosky, “An overview of dexterous manipulation,” *Proc. of the 2000 IEEE Int. Conf. Robot. Automat.*, pp. 255–262, SanFrancisco, CA, 2000.

[5] A. Bicchi, “Hands for dexterous manipulation and robust grasping: A difficult road towards simplicity,” *IEEE Trans. Robot. Automat.*, vol. 16, no. 6, pp. 652–662, 2000.

[6] D. Montana, “The kinematics of contact and grasp,” *Int. J. Robot. Res.*, vol.7, no. 3, pp. 17-32, 1988.

[7] A. Cole, J. Hauser and S. Satry, “Kinematics and control of multifingered hands with rolling contacts,” *IEEE Trans. Automat. Contr.*, vol. 34, no. 4, pp. 398–404, 1989.

[8] L. Han and J. Trincle, “Dexterous manipulation by rolling and finger gaiting,” *Proc. IEEE Int. Conf. Robot. Automat.*, vol. 1, pp. 730–735, 1998.

[9] K. Harada, M. Kaneko and T. Tsuji, “Rolling based manipulation for multiple objects,” *Proc. IEEE Int. Conf. Robot. Automat.*, vol. 4, pp. 3887–3894. 2000.

[10] S. Arimoto, P.T.A. Nguyen, H.-Y. Han and Z. Doulgeri, “Dynamics and control of a set of dual fingers with soft tips,” *Robotica*, vol. 18, no. 1, pp. 71–80, 2000.

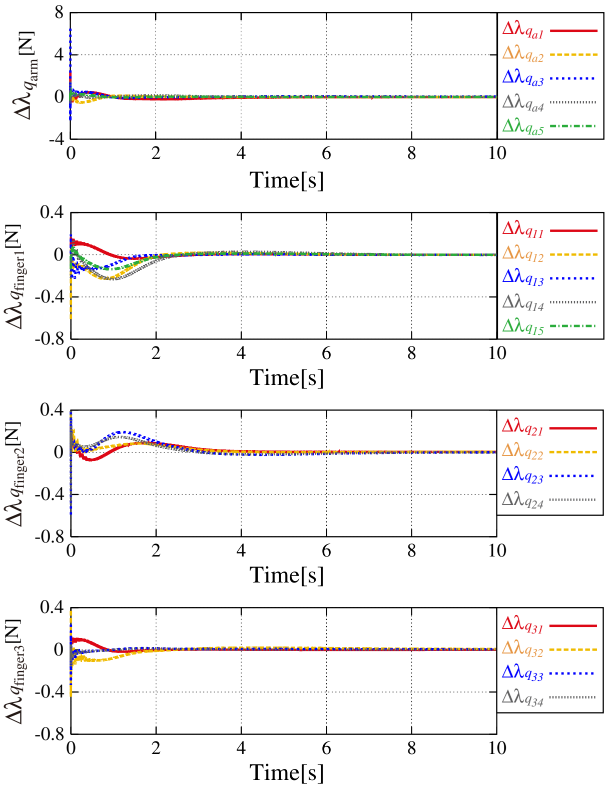

Fig. 7. Transient responses of $\Delta\boldsymbol{\lambda_q}$

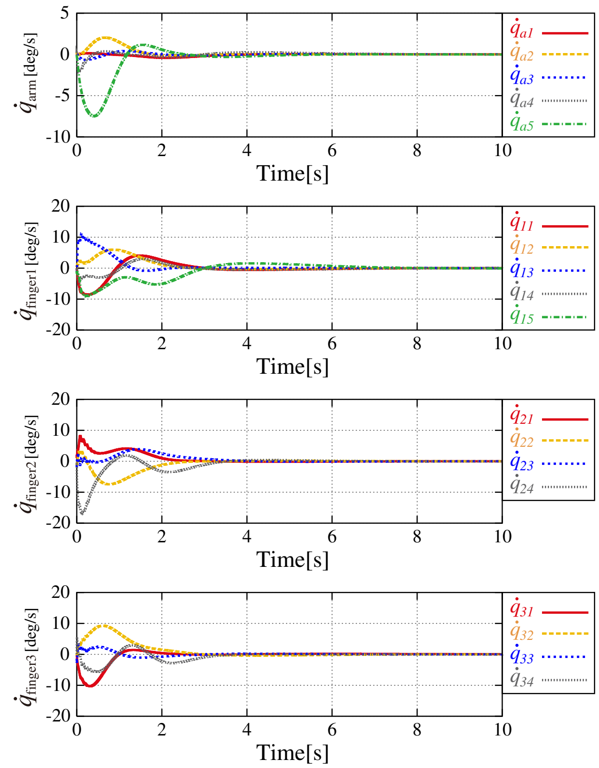

Fig. 9. Transient responses of angular velocity of the hand-arm system

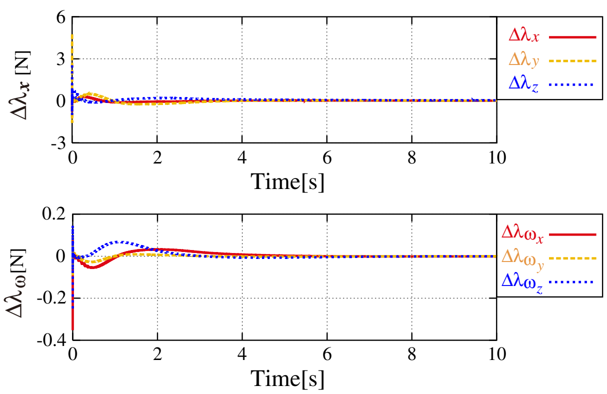

Fig. 8. Transient responses of $\Delta\boldsymbol{\lambda_x}$ and $\Delta\boldsymbol{\lambda_\omega}$

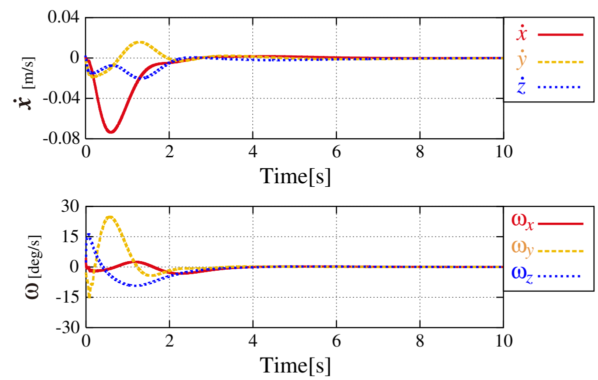

Fig. 10. Transient responses of translational and rotational velocities of the grasped object

[11] S. Arimoto, "A differential-geometric approach for 2-D and 3-D object grasping and manipulation," *Annual Review in Control*, Vol. 31, pp. 189–209, 2007.

[12] M. Yoshida, S. Arimoto and J.-H. Bae, "Blind grasp and manipulation of a rigid object by a pair of robot fingers with soft tips," *Proc. of the 2007 IEEE Int. Conf. Robot. Automat.*, pp. 4707–4714, Roma, Italy, 2007.

[13] K. Tahara, S. Arimoto and M. Yoshida, "Dynamic object grasping by a triple-fingered robotic hand," *2008 IEEE/RSJ Int. Conf. on Intelligent Robots and Systems*, pp. 2685–2690, Nice, France, 2008.

[14] A. Kawamura, K. Tahara, R. Kurazume and T. Hasegawa, "Dynamic Grasping for an Arbitrary Polyhedral Object by a Multi-fingered Hand-Arm System," *2009 IEEE/RSJ Int. Conf. on Intelligent Robots and Systems*, pp. 2264–2270, St. Louis, Missouri, 2009.

[15] M. Yoshida, S. Arimoto and K. Tahara, "Modeling and control of a pair of robot fingers with saddle joint under orderless actuations," *Proc. of the 2009 IEEE Int. Conf. Robot. Automat.*, pp. 2499–2505, Kobe, Japan, 2009.